17th World Conference on Earthquake Engineering, 17WCEE
Sendai, Japan - September 13th to 18th 2020

CONTROLLING EFFECT OF SOURCE PARAMETERS ON LOW- AND HIGH-FREQUENCY GROUND MOTIONS IN FK APPROACH

Z. Cao[(1)], X. Tao[(2)], Z. Tao[(3)]

[(1)] *PhD candidate, School of Civil Engineering, Harbin Institute of Technology, China, caozelin1990@163.com*
[(2)] *Professor, School of Civil Engineering, Harbin Institute of Technology, China, taoxiaxin@aliyun.com*
[(3)] *Professor, Institute of Engineering Mechanics, China Earthquake Administration, China, taozr@iem.ac.cn*

Abstract

We recently propose a method modeling kinematic source of a scenario earthquake for synthesis of broadband ground motion based on the frequency-wavenumber Green's function (FK approach). The kinematic source model describes the spatiotemporal rupture process with a set of source parameters, and the parameters may have different influences on the low- and high-frequency components of the synthetic ground motion. To explore the main influencing parameters at low and high frequencies respectively, this study quantitatively analyzes the sensitivity of the synthetic motion to five types of source parameters by case studies: (1) those on the occurrence of the rupture plane, including the depth and dip of the fault; (2) on the spatial variation of slip, including the size of the rupture plane, and the slip distribution; (3) on the temporal evolution of slip, including the rise time, rupture velocity and their correlation with slip, and the source time function; (4) on the randomness, including the perturbation of the rupture time, and the fault roughness expressed by the spatial randomness of slip direction, dip and strike; and (5) others, including the stress drop, the subsource size, and the constraints over the entire rupture. The results show that the low- and high-frequency ground motions are controlled by different source parameters. Generally, the temporal evolution of slip is the dominant influencing factor at high frequency, whereas the spatial variation of slip is the main influencing factor at low frequency. This study contributes to the application of the FK approach in the synthesis of broadband ground motion.

Keywords: source parameter, ground motion synthesis, FK approach, sensitivity analysis

1. Introduction

The ground motion synthesis approach based on the frequency-wavenumber Green's function (FK approach) can provide three-dimensional motions [1-4], and thus it is a promising technique for the multidimensional broadband ground motion synthesis. The FK approach obtains broadband ground motion by convolving the deterministic full-waveform Green's function with the appropriate kinematic rupture process. The kinematic source model, which describes the rupture process of an earthquake as a function of both space and time, has significant influence on the low-frequency (LF) and high-frequency (HF) synthetics [5].

In a previous study [1], we proposed a method modeling kinematic source of a scenario earthquake for the FK approach. The kinematic source model describes the spatiotemporal rupture process with a set of source parameters, including the size of the rupture plane, the slip distribution on the rupture plane and the distribution of rise time and rupture time. Further details of the source modeling method can be found in the reference [1]. These source parameters would have different influence on the LF and HF motions. Most studies on the ground motion synthesis focus on the accordance between the observations and the synthetics. For better application of the FK approach, it is necessary to analyze the influence of various source parameters on the LF and HF ground motions. This study aims to explore the source parameters controlling the LF and HF ground motions. As a preliminary study, a Mw 6.5 strike-slip earthquake is taken as a case to analyze the sensitivity of the synthetic motion to five types of source parameters. This analysis contributes to the application of the FK approach in the synthesis of broadband ground motion from past earthquakes and scenario earthquakes.

2. Analysis method

In this study, we use a simple calculation model to perform the ground motion synthesis. Fig.1 shows the fault model and the ground sites. In the model, a vertical rupture plane with size of 32×16 km^2 and depth of 5 km is set for a Mw 6.5 strike-slip earthquake. The hypocenter is set to have the unilateral rupture. Two groups of ground sites are used for calculation: Group A in the rupture forward and Group B along the perpendicular bisector of the fault projection. Each group contains 11 sites with the Joyner-Boore distances of 1, 2, 3, 5, 7, 10, 20, 30, 50, 70 and 100 km.

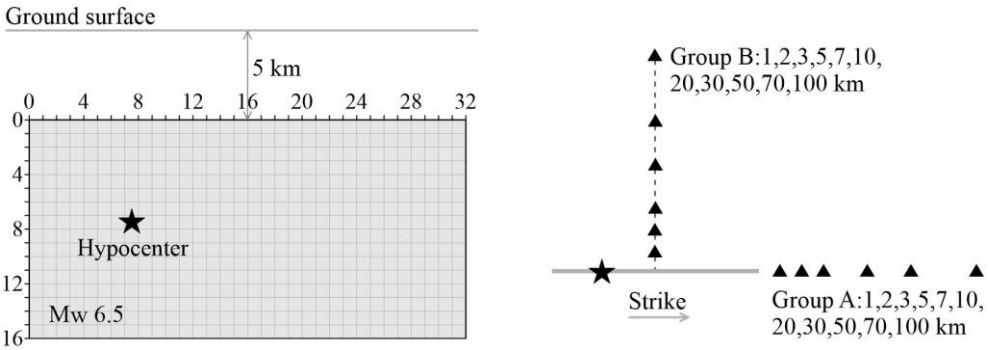

Fig. 1 – The fault model and ground sites used in this study

The reference case is taken as the basic earthquake scenario, and the corresponding source parameters are listed in Table 1. For the reference case, the distributions of slip, rupture time and rise time on the rupture plane are generated by the source modeling approach in the reference [1]. The first realization is shown in Fig.2. In the following sections, only one parameter of the reference case changes while the others keep the same. This can form a set of assumed cases for sensitivity analysis. Then, the fault-normal (FN) and fault-parallel (FP) ground motions at 22 sites for the all cases are simulated by the FK approach and band-pass filtered from 0.1 to 20 Hz.

Table 1 – Source parameters of the reference case

Source parameter	**Value**
Moment magnitude	6.5
Fault depth	5 km
Dip	90°
Rake	0°
Fault length and width	32 km×16 km
Number of subsources	32×16
Stress drop	50 bars
Perturbation of rupture time	c=0.2
Source time function	Hartzell STF [6]
Average rupture velocity	2.8 km/s

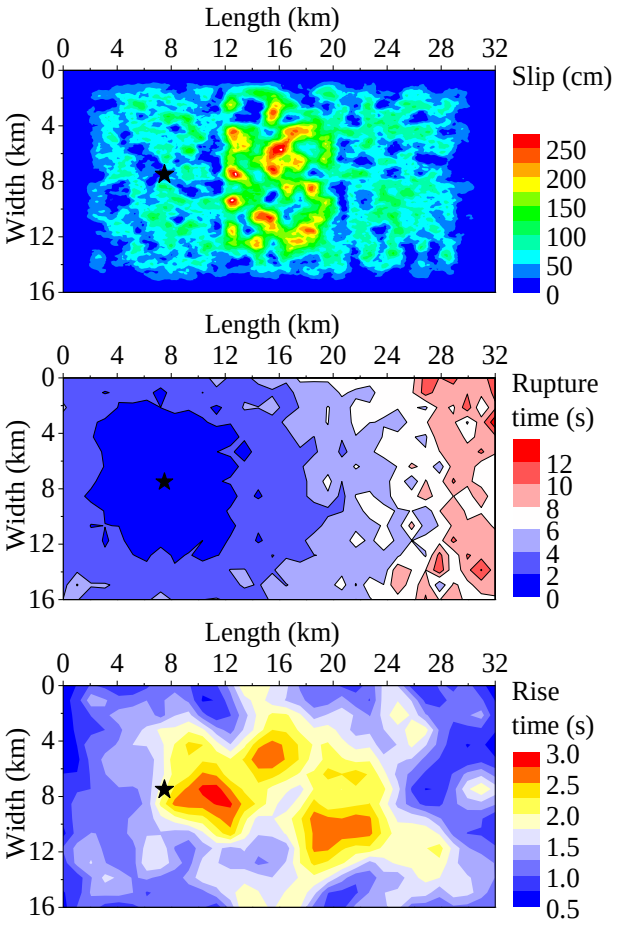

Fig. 2 – Distributions of slip, rupture time and rise time on the rupture plane

In the FK approach, the ground motion from the *ij*th subsource can be expressed by

$$a_{ij}(t) = G_{ij}(t) * STF(\tau_{ij}, t) \cdot M_{0ij} \tag{1}$$

where $G_{ij}(t)$ is the Green's function from an impulse at the *ij*th subsource; $STF(\cdot)$ is the source time function (STF); M_{0ij} and τ_{ij} are the seismic moment and rise time of the *ij*th subsource, respectively; $*$ denotes convolution; and t is the time. The Green's function is calculated by an improved frequency-wavenumber algorithm [7], and the 1D crustal structure for the Lushan region in Sichuan, China is adpoted [8]. And then the subsource motions are summed with proper time delay to obtain the ground motion from the entire rupture plane.

For each case, the 5% damped pseudo-spectral acceleration (PSA) of the RotD50 component [9] is calculated from the synthetic FN and FP motions. Then, we compute the residual at each site and the bias over all 22 sites between the RotD50 PSA of the assumed cases and that of the reference case. The bias of each set of cases can be used for quantitative analysis of the corresponding source parameter. The bias for each case is calculated by

$$B(f) = \frac{1}{N_S}\sum_{i=1}^{N_S}\left[\ln O_i(f) - \ln S_i(f)\right] \tag{2}$$

where $O_i(f)$ and $S_i(f)$ are PSA at the *i*th site of the assumed case and of the reference case, respectively; f is frequency; and N_S is the number of sites. For the reference case, the bias would be 0; for each assumed case, a positive value would indicate larger estimation, and smaller bias difference means slight influence of source parameter on the synthetic motion.

3. Sensitivity to occurrence of rupture plane

The fault depth and dip control the occurrence of the rupture plane. In this section, the fault depth is set as 1, 3, 5, 7 and 9 km, and the other parameters keep the same. Then, ground motions at all 22 sites for these five assumed cases are synthesized, and the bias values for each case are computed by Eq. (2). Fig.3 shows the bias versus frequency. It can be seen that with the increase of fault depth, both the LF and HF motions decrease clearly. This result is consistent with the expectation that larger depth causes stronger attenuation and thus smaller ground motion.

To check the influence of dip, the dip angles of 30°, 45°, 60°, 75° and 90° are set for different assumed cases, and the other parameters keep the same. The projection of the center of fault and the locations of sites are fixed. Fig.4 shows the corresponding biases. Generally, the influence of dip on the LF and HF ground motions is quite small. As the focal mechanism keeps the same, the influence of dip is equivalent to the influence of subsource-to-site distance. It is expected that the influence is larger in near field and smaller in far field. As the ground points are distributed in a wide distance range, the average influence is small.

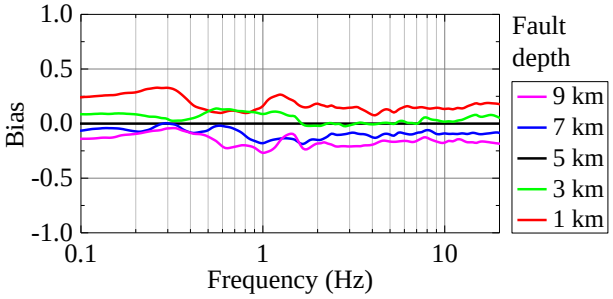

Fig. 3 – Influence of fault depth on ground motion

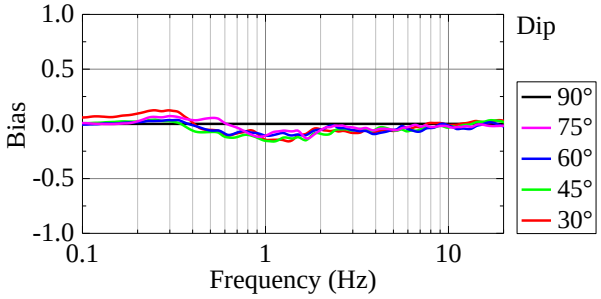

Fig. 4 – Influence of dip on ground motion

To further investigate the variation of the influence, Fig.5 shows the absolute value of the residual in each group of sites versus the Joyner-Boore distance for the cases with fault depth of 1 km and with dip of 30°. In Fig.5, two groups of sites are analyzed separately, the LF and HF residuals are the averages of 3.0-5.0 s and 0.3-0.5 s, respectively. For the fault depth, the influence at HF is smaller than that at LF. In the near field, the influence is complex because of the significant effect of source-to-site distance. The influence decreases with distance for Group B at distances above 10 km and for Group A below 30 km. The increase of residual for Group A above 30 km is due to the reflection of seismic waves at the interfaces in the crust. The influence of dip is complex in the near-fault region and then decreases with distance.

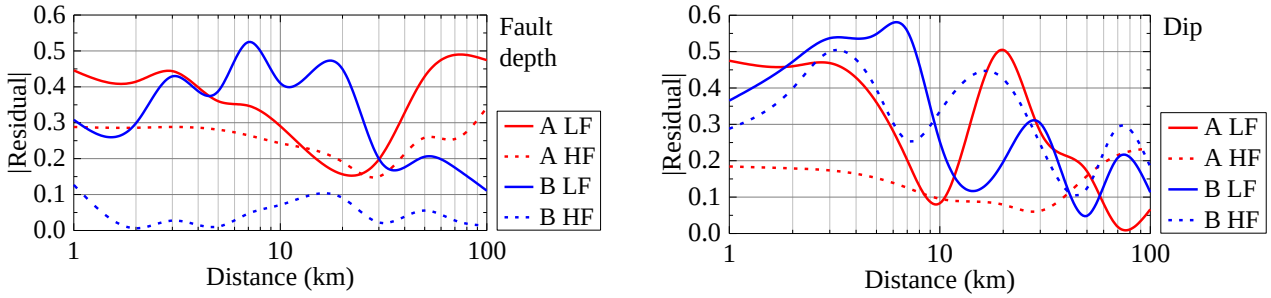

Fig. 5 – Variation of the absolute residual versus distance for fault depth of 1 km and for dip of 30°

4. Sensitivity to spatial variation of slip

Source parameters describing the spatial variation of slip are generally grouped into two categories: the size of the rupture plane and the nonuniform slip distribution on the rupture plane. In the FK approach, the size of the rupture plane and the slip distribution are estimated based on the scaling laws of source parameters.

For an earthquake with a given magnitude, the size of the rupture plane may vary in a certain range. For simplicity, the size of the rupture plane is set as 28×12, 30×14, 32×16, 34×18 and 36×20 km^2 to check its influence. For this set of assumed cases, the pattern of slip distribution keeps the same, whereas the rupture time and rise time change. The biases for each case are compared in Fig.6. It is clear that the synthetic ground motion decreases with the size of the rupture plane, and the influence is much significant at LF and relatively small at HF. With the same magnitude, smaller rupture plane indicates smaller rupture time, and thus, produces stronger motion.

For the source modeling, the slip distribution and the corresponding rise time and rupture time are different in each realization. In addition to the first realization shown in Fig.2, we use another four simulations to check the influence of slip distribution on the synthetic ground motion. The bias plots in Fig.7 indicate that the bias difference is large at LF and quite small at HF. As the constraint on rise time in FK approach is very strong, the slip distribution nearly has no influence on the HF spectral level.

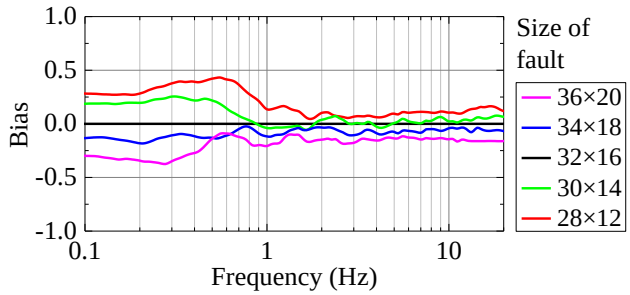

Fig. 6 – Influence of size of fault on ground motion

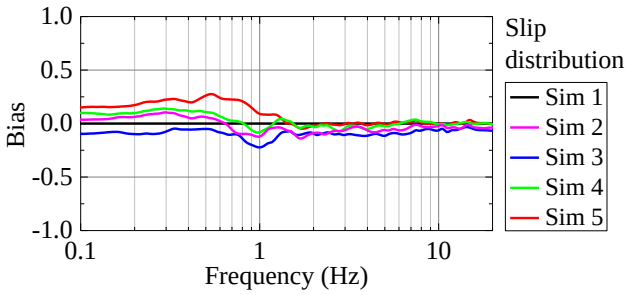

Fig. 7 – Influence of slip distribution on ground motion

5. Sensitivity to temporal evolution of slip

The temporal evolution of slip is determined by three parameters: the source time function (STF), rise time and rupture velocity. The rupture process for each subsource is parameterized as the same STF with variable rise time and seismic moment, and the rupture velocity governs the time delay of the triggering of each subsource.

The rise time is defined as the time for slip to reach its final value from zero at a point on the rupture plane during an earthquake; its frequency-domain equivalent is the corner frequency of the source radiation spectrum [10]. We set the rise time to be 0.5, 0.75, 1.0, 1.5, and 2.0 times the value of the reference case, and the other parameters keep the same. Fig.8 shows the bias values for these cases. The bias significantly increases with the decreasing rise time, and this is because that the HF spectral amplitude increases with the corner frequency (the reciprocal of rise time). The bias difference at HF is more significant than that at LF, and the influence of rise time is much larger than those of other parameters. Thus, it is very important to properly generate and constrain the rise time.

For a given slip distribution, the rise time is different in each simulation due to the randomness. We use five simulations to check the influence of the randomness of rise time. The rise time is different whereas the others keep the same. The results shown in Fig.9 indicate that the influence is very small at HF and slightly larger at LF. Although the distribution of rise time on the rupture plane is different, the strong constraint on the rise time over the entire rupture plane ensures that the source model produces similar HF ground motion.

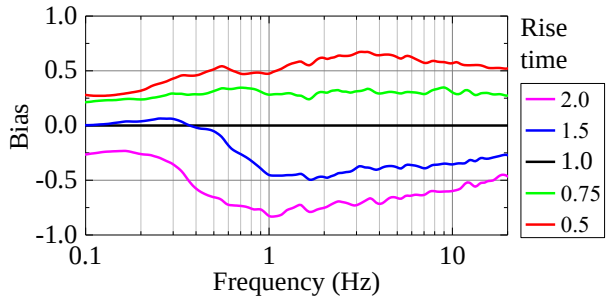

Fig. 8 – Influence of the rise time on ground motion

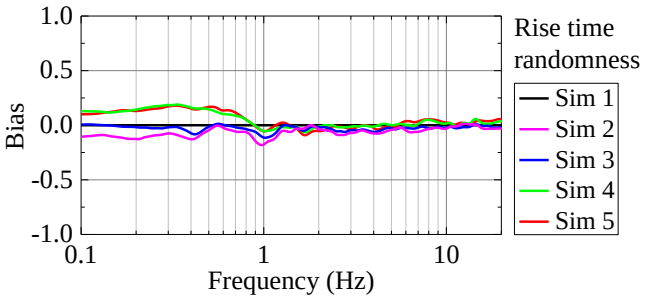

Fig. 9 – Influence of the randomness of rise time on ground motion

The rupture velocity controls the triggering of the rupture at all points and is critical in summing the time histories from subsources. The FK approach uses a uniform distribution on [0.6, 1.0] to generate the ratio of the local rupture velocity to the local shear-wave velocity. The local rupture velocity is preliminarily determined from the product of this ratio with the local shear-wave velocity and is then rescaled to the expected average value of 2.8 km/s. The initial rupture time of each subsource is calculated from the distribution of the local rupture velocity and the hypocenter. Then, a random perturbation is added to the initial rupture time to consider the incoherence of the rupture front by using the following formula

$$t_{ij} = t_{ij}^{0} \exp(c\zeta) \tag{3}$$

where t_{ij}^{0} and t_{ij} represent the initial and perturbed rupture times of the ijth subsource, respectively; c is set to 0.2; and ζ is a random number subject to the standard normal distribution. The multiplication in Eq. (3) ensures that the perturbation increases with the initial rupture time.

The average rupture velocity across the entire rupture plane is set as 2.2, 2.5, 2.8, 3.1 and 3.4 km/s. The bias plots in Fig.10 show that the differences are quite small at HF and relatively large at LF. As expected, a larger average rupture velocity causes a smaller rupture time, and thus, stronger motion. For each

simulation, the rupture time is different due to the randomness of the rupture velocity and the perturbation. We use five simulations to check the influence of the randomness of rupture time. The rupture time is different whereas the others keep the same. The results shown in Fig.11 indicate that the influence is evident at LF and quite small at HF. Therefore, in the FK approach, the estimation of the average rupture velocity and the randomness of rupture time is important for LF synthetics.

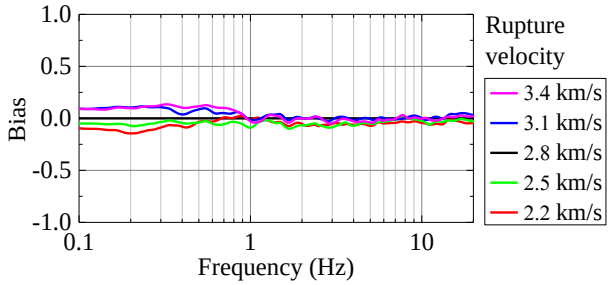

Fig. 10 – Influence of the average of rupture velocity on ground motion

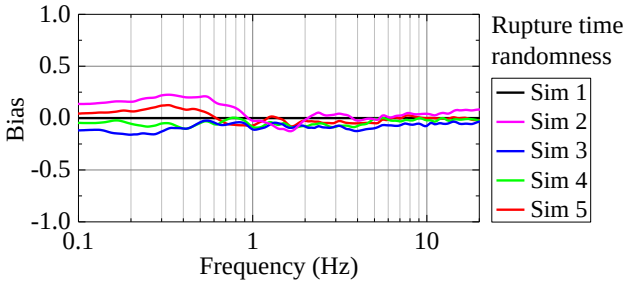

Fig. 11 – Influence of the randomness of rupture time on ground motion

A credible STF model serves as a proxy for the slip process at each subsource. To date, various analytical functions for STFs have been introduced, including simple mathematical functions and more complicated pseudo-dynamic functions. Here we choose five STFs to examine the sensitivity: the Boxcar STF, the Triangular STF, the Hartzell STF [6], the Brune STF [11] and the Liu STF [12]. The other parameters keep the same. The bias plots in Fig.12 indicate that the STF has great influence on the synthetic ground motion, as presented below.

Generally, the Boxcar STF, the Triangular STF and the Hartzell STF produce similar LF ground motion, whereas the Brune STF and the Liu STF have close LF synthetics. The difference at LF between two sets of STFs may be due to the difference of the definition of rise time. At HF, the result of the Triangular STF is close to that of the Hartzell STF, and that of the Boxcar STF increases with frequency; the Brune STF and the Liu STF still produce much larger HF ground motion. The difference at HF can be partly attributed to the differences in the Fourier spectra of STFs. Besides the rise time, the STF has the largest influence on ground motion. Based on the analysis of spectral hole, HF spectral decay rate and the compatibility with the rupture dynamics, the Hartzell STF is recommended for predicting strong motions [1].

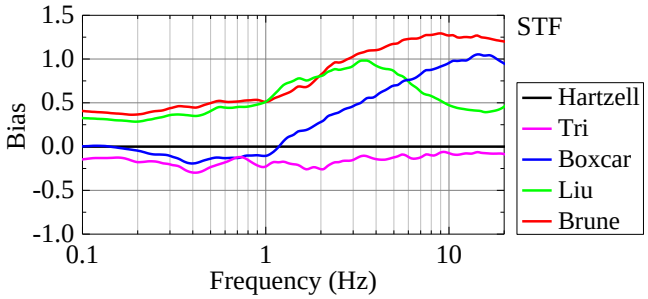

Fig. 12 – Influence of the source time function on ground motion

6. Sensitivity to other parameters

The perturbation of rupture time affects the final rupture time and thus the synthetic motion. For Eq. (3), we set the parameter c as 0, 0.1, 0.2, 0.3 and 0.4 to have different perturbations. The rupture time changes whereas the other parameters keep the same. The corresponding biases are plotted in Fig.13. It is clear that

the perturbation of rupture time has little influence on HF motion and significant influence on LF motion. And the LF motion increases with decreasing *c*. Fig.15 shows the velocity and acceleration time histories of FN component at site A20 for different perturbations of rupture time. For the pure strike-slip rupture, it is expected that site A20 would exhibit large velocity pulse in FN component. With the increase of *c*, the perturbation of rupture time increases significantly, and the amplitude and waveform of velocity have great change. Too large perturbation would cause unreasonable rupture time, and it is harmful to the synthesis of LF velocity pulse. For the acceleration time history, too large perturbation causes large duration of time history. In fact, the parameters related to the rupture time influence the summation of subsource motions and the coherence of LF motion. For the broadband synthesis using the FK approach, it is necessary to further investigate the randomness and perturbation of rupture time.

The rupture plane is usually not smooth, and this may influence the HF seismic waves as the small-scale affects the propagation of the seismic waves with short wavelength. In the FK approach, the roughness of the rupture plane is expressed by the frequency dependency of dip, rake and subsource-to-site azimuth of each subsource [13]. The maximum disturbance values of three parameters are 30°, 40° and 50°, respectively. We set the maximum disturbance values to be 0, 0.5, 1.0, 1.5 and 2.0 times the original values to obtain different degrees of roughness of the rupture plane, and the other parameters keep the same. The bias plots in Fig.14 indicate that the HF motion slightly decreases with the roughness and the LF motion has little variation. This is because that larger roughness results in smaller difference between FN and FP motions, and thus, the RotD50 PSA would also decrease. For future study on the relationship between FN and FP synthetics, the roughness needs further analysis.

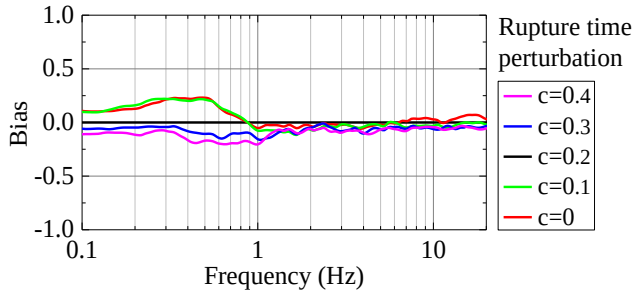

Fig. 13 – Influence of the perturbation of rupture time on ground motion

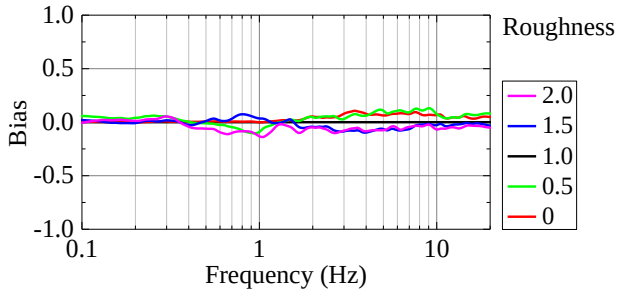

Fig. 14 – Influence of the roughness of the rupture plane on ground motion

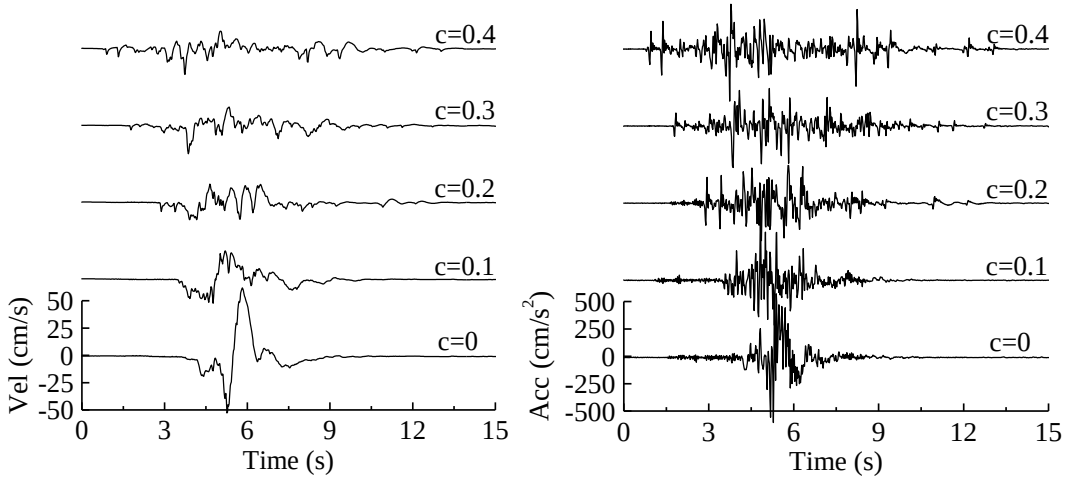

Fig. 15 – Velocity and acceleration time histories of FN component at site A20 for different *c*

In the FK approach, the stress drop controls the rise time and thus the HF spectral amplitude. We set the stress drop to be 1/3, 1/2, 1, 2 and 3 times the value in Table 1. In these cases, the rise time changes and the other parameters keep the same. The biases shown in Fig.16 indicate that the influence is very small at LF and significant at HF. The synthetic motion increases with the stress drop, and this is similar as Fig.8.

A source model should keep the synthetics independent of the subsource discretization scheme. To test the performance of the FK approach, we divide the entire rupture plane into 8×4, 16×8, 32×16, 64×32 and 128×64 subsources, generate the rise time and rupture time and then synthesize ground motions. The bias plots in Fig.17 show that the HF motions are quite close and the LF motions have slight difference. The LF motion of the 128×64 subsources is smaller than those of others. This is because that for the finer discretization, the influence of the perturbation of rupture time significantly increases, as presented in Fig.13. If there has no perturbation of rupture time, the results of different discretization schemes would be very close over the whole frequency range.

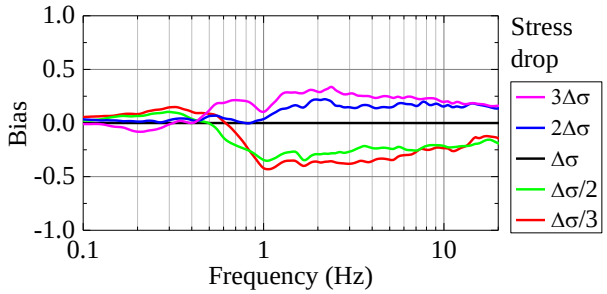

Fig. 16 – Influence of the stress drop on ground motion

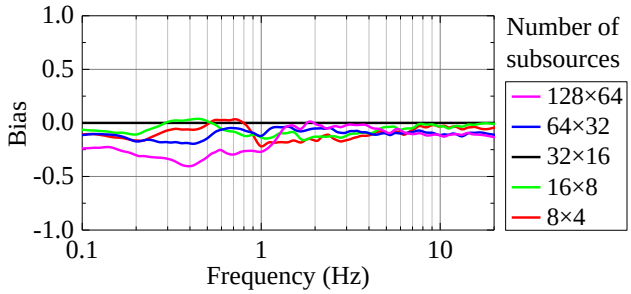

Fig. 17 – Influence of the number of subsources on ground motion

7. Conclusions

This study systematically investigates the sensitivity of the synthetic motion to various source parameters, including those on the occurrence of the rupture plane, on the spatial variation and temporal evolution of slip and on the randomness and roughness of the rupture plane. As a preliminary study, a Mw 6.5 strike-slip earthquake is adopted to set different cases, the broadband ground motions for each case are simulated using the FK approach, and then the bias of RotD50 PSA over all 22 sites is used for quantitative analysis.

For the occurrence of the rupture plane, both the LF and HF motions decrease clearly with the fault depth, and the influence of dip on the LF and HF motions is quite small. The influence of the depth and dip is equivalent to the influence of subsource-to-site distance. Generally, the influence decreases with distance in far field. For the spatial variation of slip, the synthetic motion decreases with the size of the rupture plane, and this influence is much significant at LF and relatively small at HF. The influence of slip distribution is large at LF and quite small at HF. For the temporal evolution of slip, the synthetic motions significantly increase with the decreasing rise time and the rise time has the largest influence on the synthetic motion among all source parameters. Under the constraint of rise time in the FK approach, the influence of the randomness of rise time is very small at HF and slightly larger at LF. The STF has great influence on the synthetic ground motions, especially the HF components. From the results regarding the temporal evolution and the spatial variation of slip, the temporal evolution of slip is the dominant influencing factor at HF, whereas the spatial variation of slip is the main influencing factor at LF. This is consistent with a previous theoretical analysis [14]. Besides, both the average value of the rupture velocity and the perturbation of the rupture time have weak influence at HF and strong influence at LF. The perturbation of the rupture time affects the coherence of subsource motions and the LF synthetics. In addition, the roughness slightly affects the HF motion, the influence of the stress drop is very small at LF and significant at HF, and the source modeling can keep the synthetics independent of the subsource discretization scheme. The results obtained in this study can be used for application of the FK approach for broadband ground motion synthesis.

8. Acknowledgements

The authors gratefully acknowledge the financial support from the National Natural Science Foundation of China (Grant Nos. 51778197, 51678540, 51478443).

9. Copyrights

10. References

[1] Cao Z, Tao X, Tao Z, Tang A (2019): Kinematic source modeling for the synthesis of broadband ground motion using the *f-k* approach. *Bulletin of the Seismological Society of America*, **109** (5), 1738-1757.

[2] Hartzell S, Guatteri M, Mai PM, Liu P, Fisk M (2005): Calculation of broadband time histories of ground motion, Part II: Kinematic and dynamic modeling using theoretical Green's functions and comparison with the 1994 Northridge earthquake, *Bulletin of the Seismological Society of America*, **95** (2), 614-645.

[3] Kieling K, Wang R, Hainzl S (2014): Broadband ground-motion simulation using energy-constrained rise-time scaling. *Bulletin of the Seismological Society of America*, **104** (6), 2683-2697.

[4] Crempien JGF, Archuleta RJ (2015): UCSB method for simulation of broadband ground motion from kinematic earthquake sources. *Seismological Research Letters*, **86** (1), 61-67.

[5] Cao Z, Tao X (2018): Review on broadband ground motion simulation based on frequency-wavenumber Green's function. *Earthquake Engineering and Engineering Dynamics*, **38** (5), 33-40. (in Chinese)

[6] Hartzell S, Liu P, Mendoza C, Ji C, Larson KM (2007): Stability and uncertainty of finite-fault slip inversions: Application to the 2004 Parkfield, California, earthquake. *Bulletin of the Seismological Society of America*, **97** (6), 1911-1934.

[7] Zhu L, Rivera LA (2002): A note on the dynamic and static displacements from a point source in multilayered media. *Geophysical Journal International*, **148** (3), 619-627.

[8] Hao J, Ji C, Wang W, Yao Z (2013): Rupture history of the 2013 Mw 6.6 Lushan earthquake constrained with local strong motion and teleseismic body and surface waves. *Geophysical Research Letters*, **40** (20): 5371-5376.

[9] Boore DM (2010): Orientation-independent, nongeometric-mean measures of seismic intensity from two horizontal components of motion. *Bulletin of the Seismological Society of America*, **100** (4), 1830-1835.

[10] Beresnev IA (2002): Source parameters observable from the corner frequency of earthquake spectra. *Bulletin of the Seismological Society of America*, **92** (5), 2047-2048.

[11] Brune JN (1970): Tectonic stress and the spectra of seismic shear waves from earthquakes. *Journal of Geophysical Research*, **75** (26), 4997-5009.

[12] Liu P, Archuleta RJ, Hartzell S (2006): Prediction of broadband ground-motion time histories: Hybrid low/high-frequency method with correlated random source parameters. *Bulletin of the Seismological Society of America*, **96** (6), 2118-2130.

[13] Pitarka A, Somerville P, Fukushima Y, Irikura K (2000): Simulation of near-fault strong-ground motion using hybrid Green's functions. *Bulletin of the Seismological Society of America*, **90** (3), 566-586.

[14] Beresnev IA (2017): Factors controlling high-frequency radiation from extended ruptures. *Journal of Seismology*, **21** (5), 1277-1284.

